Elemental Scientific
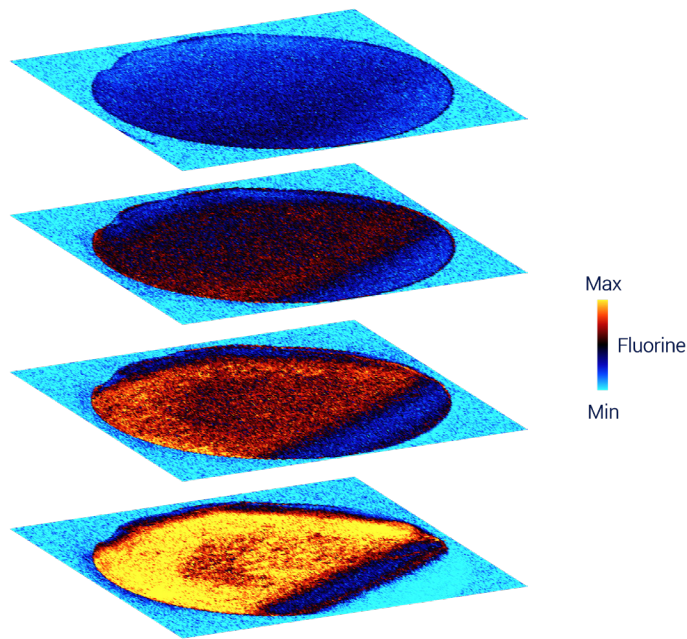**L A S E R S**
INNOVATION TO ILLUMINATE

Authors: Ross Coenen[1], Lisa Balke[2], Josh Stone[3], Uwe Karst[2], C. Derrick Quarles Jr.[1]

Elemental Imaging of Anodes from Cycled Lithium-ion Batteries

imageGEO[LIBS], ESLumen, iLumen

Surface Layer

Max

Fluorine

Min

3D representation of the F signal per layer for the 3.6V anode (Fig. 9, pg. 9).

Brief

Laser-induced breakdown spectroscopy (LIBS) was used to investigate the elemental distribution within the solid-electrolyte interphase (SEI) of the lithium-ion batteries. Four different anodes were analyzed in this study, these were a pristine, 3.6V, 3.6V without fluoroethylene carbonate (FEC), and 4.8V. Each battery was cycled (charge/discharge) three times each.

Highlights

- Simultaneous determination of Li, Na, C, F, Mn, Ni, Co, and O within the SEI using LIBS

- LIBS offers the unique ability to detect elements such as F, O, and H

- Elemental maps (e.g., Li, F, etc.) comparing cycle voltages

- Detection of Ni, Mn, and Co on the anode surface after over cycling at 4.8V

1. Elemental Scientific, Inc., Omaha, NE, USA
2. University of Muenster, Muenster, Germany
3. Elemental Scientific Lasers, Bozeman, MT, USA

Introduction

Lithium-ion batteries have become the main source for portable electric energy, due to their compact size and high energy density. Lithium-ion batteries supply long-lasting power making them ideal for phones, computers, and electric vehicles (EVs). Improving performance, while maintaining safety, has become an important factor driving the production of these devices. The solid-electrolyte interphase (SEI), which forms on the anode surface, plays an important part in the battery efficiency and longevity. The SEI layer generally consists of degradation products from the electrolyte, which typically comprises the elements Li, F, C, H, and O. Elemental imaging using traditional techniques, such as inductively coupled plasma mass spectrometry (ICPMS), does not provide the ability to detect H and O since it is an atmospheric plasma. Additionally, since it is an argon-based plasma, it does not have a high enough ionization potential (Ar = 15.2 eV) to excite F (17.4 eV). Laser-induced breakdown spectroscopy can detect F when it is performed in a helium (24.6 eV) purged chamber. In addition, by purging the chamber with gas all atmospheric air is removed, making it possible to detect and quantify O, H, and N. Therefore, LIBS provides the ability to detect all the elements of interest in anode and cathode-based materials.

Experimental

All analyses were performed with the imageGEO^{LIBS}. The imageGEO^{LIBS} consist of a 193 nm ArF excimer laser, a two-volume (TwoVol3, TV3) laser ablation cell, and is operated using ActiveView2 (AV2) software. The TV3 has two LIBS ports for light collection into the ESLumen and iLumen, which is illustrated in Figure 1. The ESLumen is a multi-channel spectrometer with CMOS detectors and the iLumen is a high-resolution spectrometer with an ICCD detector. When the laser fires upon a given sample, a small amount of material (fg to pg) is removed. This material is vaporized, atomized, and excited within the laser-induced plasma. Once this plasma begins to cool, light is emitted (µs time frame) which can be collected by the spectrometers. Every element on the periodic table emits light at one or more characteristic wavelengths, providing element-specific information with each laser pulse. When an ICP or ICPMS is connected to the TV3, particles can be transported from the laser ablation event to the ICP or ICPMS resulting in LA-ICP or LA-ICPMS measurements. LA-ICP or LA-ICPMS was not performed in this work, but could be used additionally in these types of applications for a more sensitive detection of minor elements in the SEI. Unlike bulk digestion methods, LIBS and LA-ICPMS provide spatially resolved information about a given sample. Each sample was analyzed using 100+ raster line scans with no overlapping laser shots. These line scans contain spatial information which, along with

Table 1. imageGEO^{LIBS} operating parameters.

Laser Spot Size	150 µm
Laser Dosage	1 (No overlap)
Laser Fluence	4.5 J/cm^2
Laser Repetition Rate	85 Hz
Stage Speed	4250 µm/s
Gas Flow Rate	1.0 L/min helium
ESLumen Spectrometer Delay	0.25 µs
ESLumen Integration Time	200 µs
iLumen Spectrometer Delay	0.25 µs
iLumen Integration Time	500 µs
iLumen Intensifier	5X

the LIBS elemental information, were used to construct 2D images using iolite V4.8. The anodes were ablated consecutively until the Cu current collector was reached to create depth profiles. The sample was refocused after each pattern (+100 lines scans) and repeated to obtain depth information with each succeeding pattern collected. Instrument parameters can be found in Table 1.

In this work, four different graphite anodes were investigated: pristine anode (raw anode material, never assembled into a battery), anode charged to 4.8V, and two anodes charged to 3.6V (one without fluoroethylene carbonate (FEC) and one with FEC added to the electrolyte). Figure 2 displays an optical image of the pristine, 3.6V, and 4.8V anodes, which were cycled 3 times (charge/discharge). The anodes were made of graphite (SMGA5), cathodes were made of NMC622 (lithium: nickel: manganese: cobalt; 6:2:2 ratio). The electrolyte was made up of LP57 (30:70 wt% ethylene carbonate (EC):ethyl methyl carbonate (EMC)), 1 M $LiPF_6$, and 5 wt% FEC. As noted above, one battery did not include FEC in the electrolyte during cycling and is labeled as 3.6V w/o FEC in the results to follow.
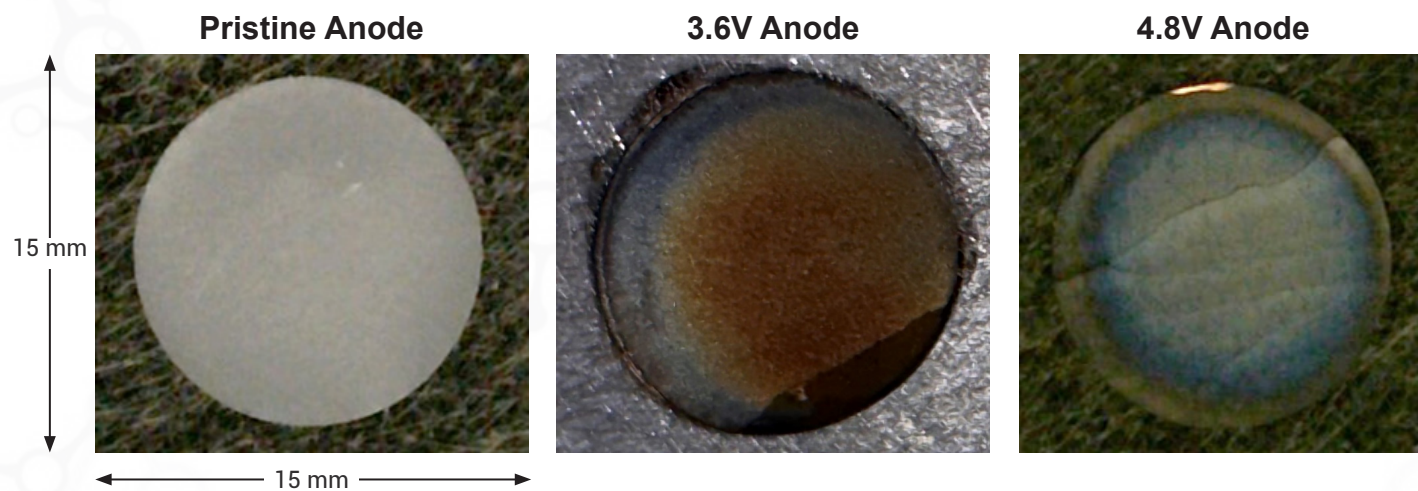
Pristine Anode	3.6V Anode	4.8V Anode

Figure 2. Image of the pristine, 3.6V, and 4.8V anodes prior to laser ablation. The anodes are ~ 15 mm in diameter. The 3.6V and 4.8V anodes were cycled with LP57 + FEC electrolyte.
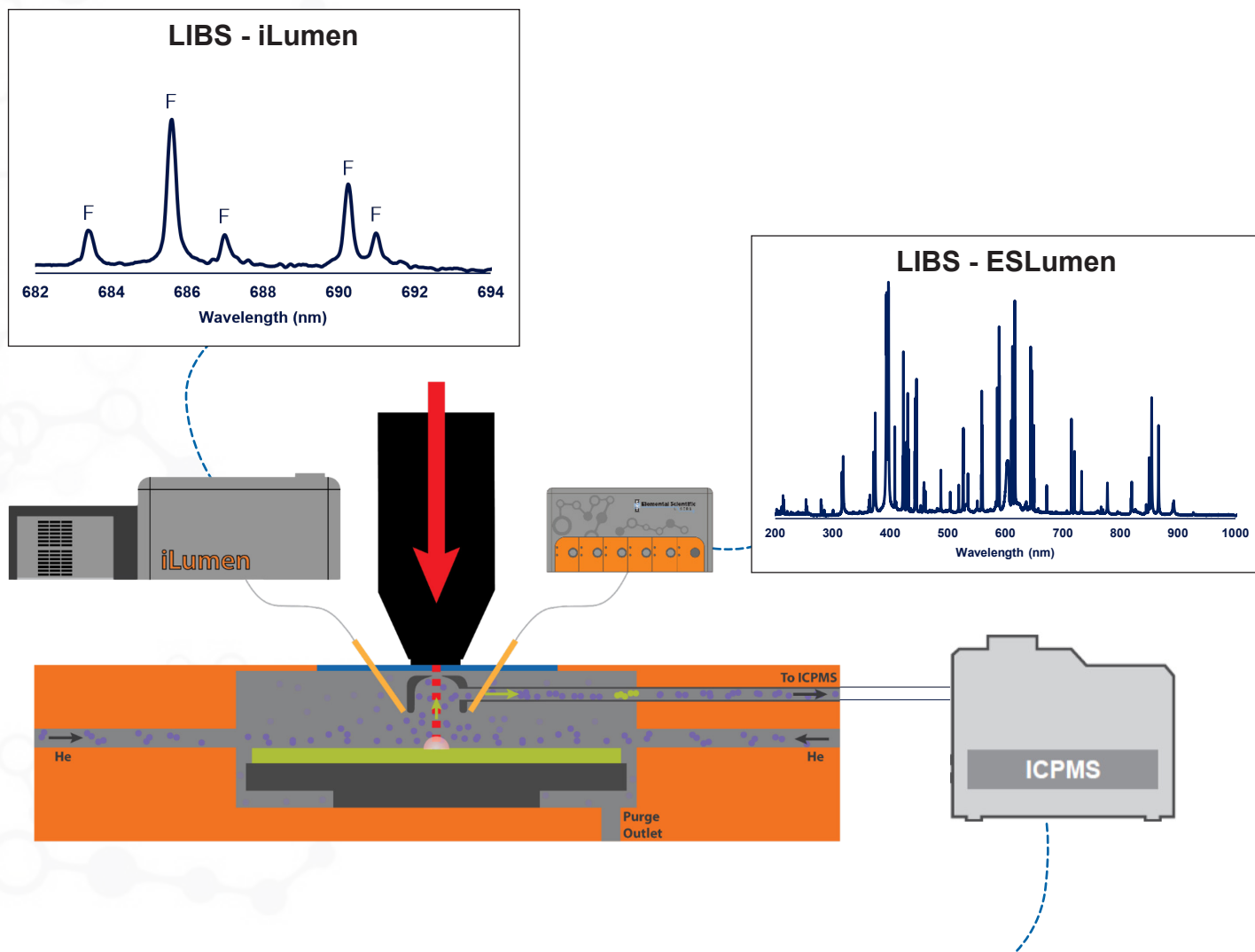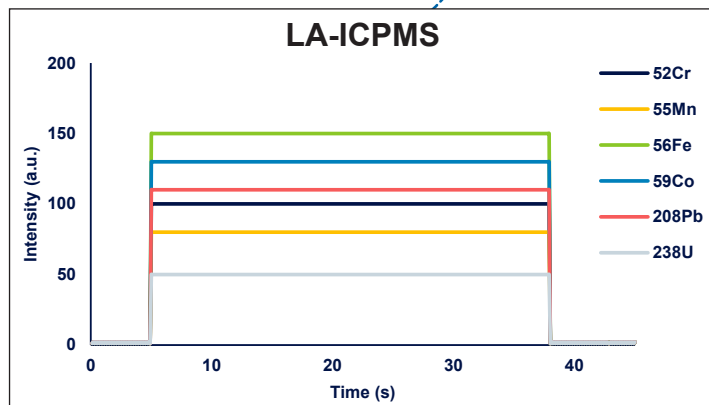
Figure 1. Illustration of the imageGEO TV3 setup with two LIBS ports connecting to the ESLumen and iLumen. ICPMS was not utilized in this work, however, LA-ICPMS could be implemented using the same setup for battery related applications.

Results

Batteries were cycled to 3.6 or 4.8V, then disassembled and the anodes were analyzed by LIBS. Figure 3 displays an illustration of the charged and discharged state of the batteries. During charging, the Li ions migrate towards the anode, whereas, during discharge, the Li ions move back towards the cathode. In this work, we wanted to investigate the effects on the anode material from normal and over-cycling of the batteries. It has been shown previously that the metal ions from the cathode can be found deposited on the anode surface if the voltage exceeds what is considered normal limits. Analysis of the 4.8V anode displayed these same trends. Figure 4 displays a LIBS spectrum highlighting the expected elements (Li, Na, F, C) in the anode material as well as the metal ions (Ni, Mn, Co) from the cathode material that deposited on the anode surface.

Figure 3. Illustration of how the Li ions migrate during a) charging and b) discharging.
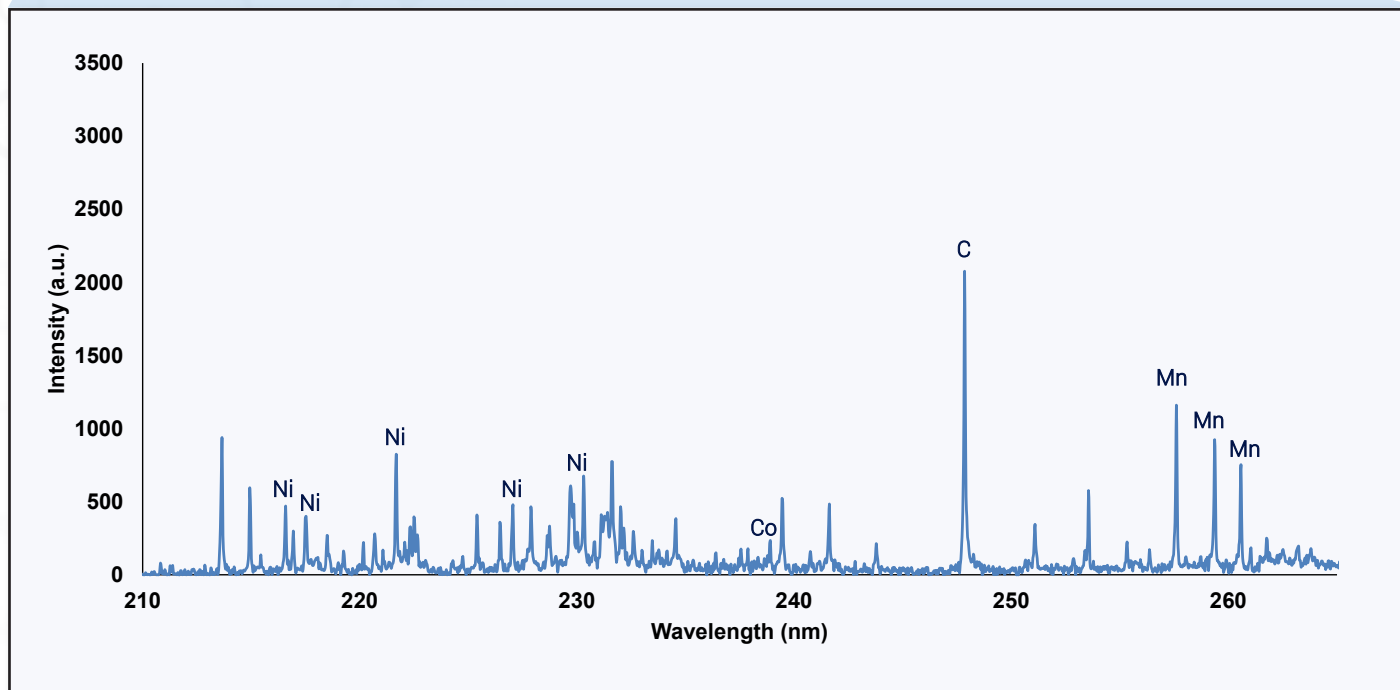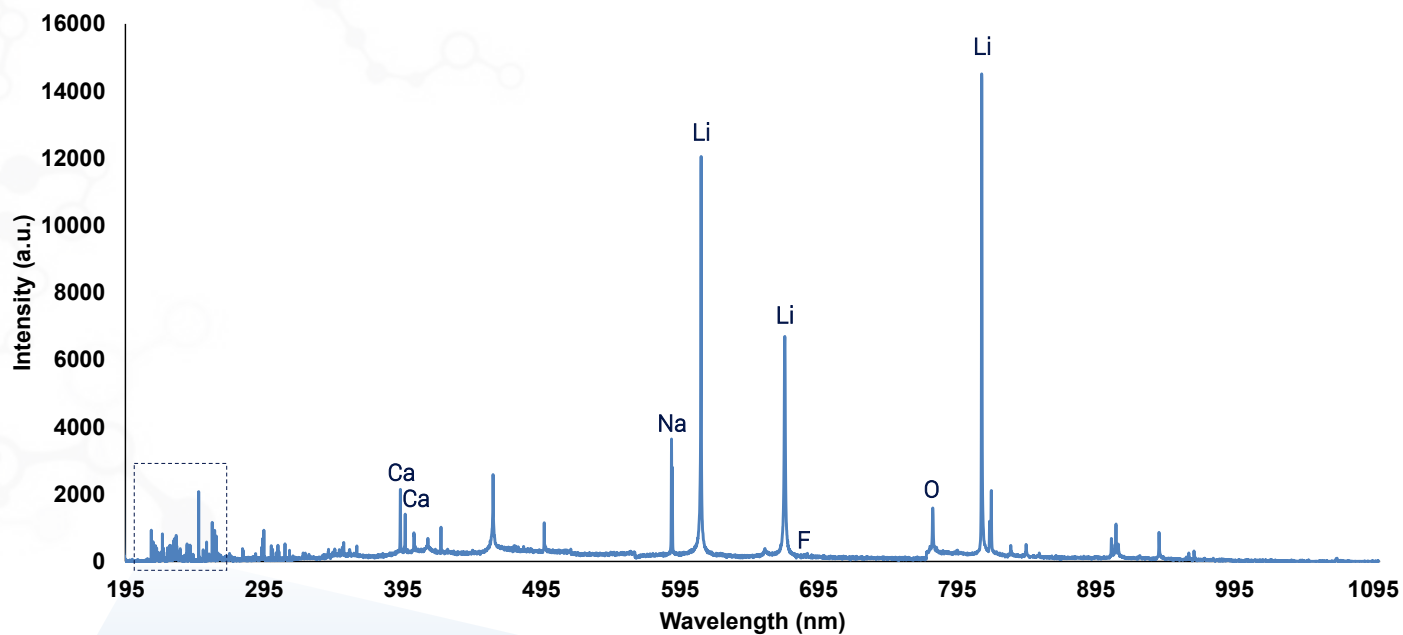
Figure 4. Displays a LIBS spectrum from the surface of the 4.8V anode (cycled 3 times) collected with the ESLumen.

Figure 5 displays the elemental images for the surface of the pristine, 3.6V, and 4.8V anodes. The pristine anode contained Na, F, and C, which represent the PVDF binder (Na and F) and the graphite material (C). The 3.6V contained the same elements with the addition of Li, which comes from charging the battery. The F signal is higher in the 3.6V anode as compared to the pristine anode, which is most likely deposition of F from the $LiPF_6$ electrolyte. The C and Na signals are lower in the 3.6V anode as compared to the pristine anode, this is likely due to the SEI layer formation on the surface that is coating the top layer which reduces the signals. When looking at the 4.8V data, there is more of a decrease in the Na and C signals as compared to the pristine and 3.6V anode. In addition, it is evident in Fig. 5 that the overcycling has led to deposition of the cathode material (Ni, Mn, Co, O) on the surface of the anode.
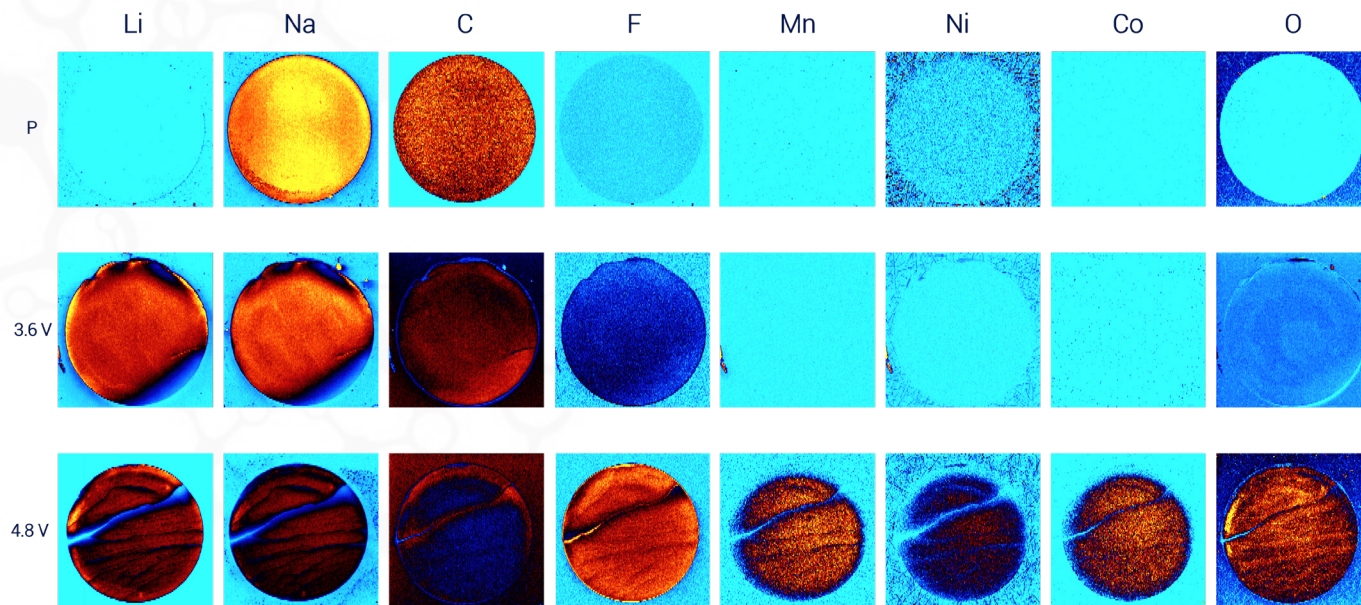

Figure 5. Elemental maps of the surface from pristine, 3.6V, and 4.8V anodes for Li, Na, C, F, Mn, Ni, Co, and O.
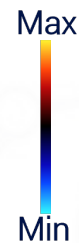
Figure 6 displays how the top three layers vary in response for Li, Na, C, and Ni between the pristine, 3.6V, and 4.8V anodes. The Li, C, and Na responses level off to about the same response once we get below the SEI layer for the 3.6V and below the SEI layer + NMC deposition for the 4.8V. All the elemental maps of layers 1 − 3 for the 3.6V and 4.8V anodes can be found in Fig. 7 and Fig. 8, respectively. The 3.6V anode does not show any Ni, Mn, or Co on the top layer or beneath the surface. The 4.8V anode has the highest amount of the cathode material (Ni, Mn, and Co) on the top layer, with it decreasing as we analyze deeper into the anode.
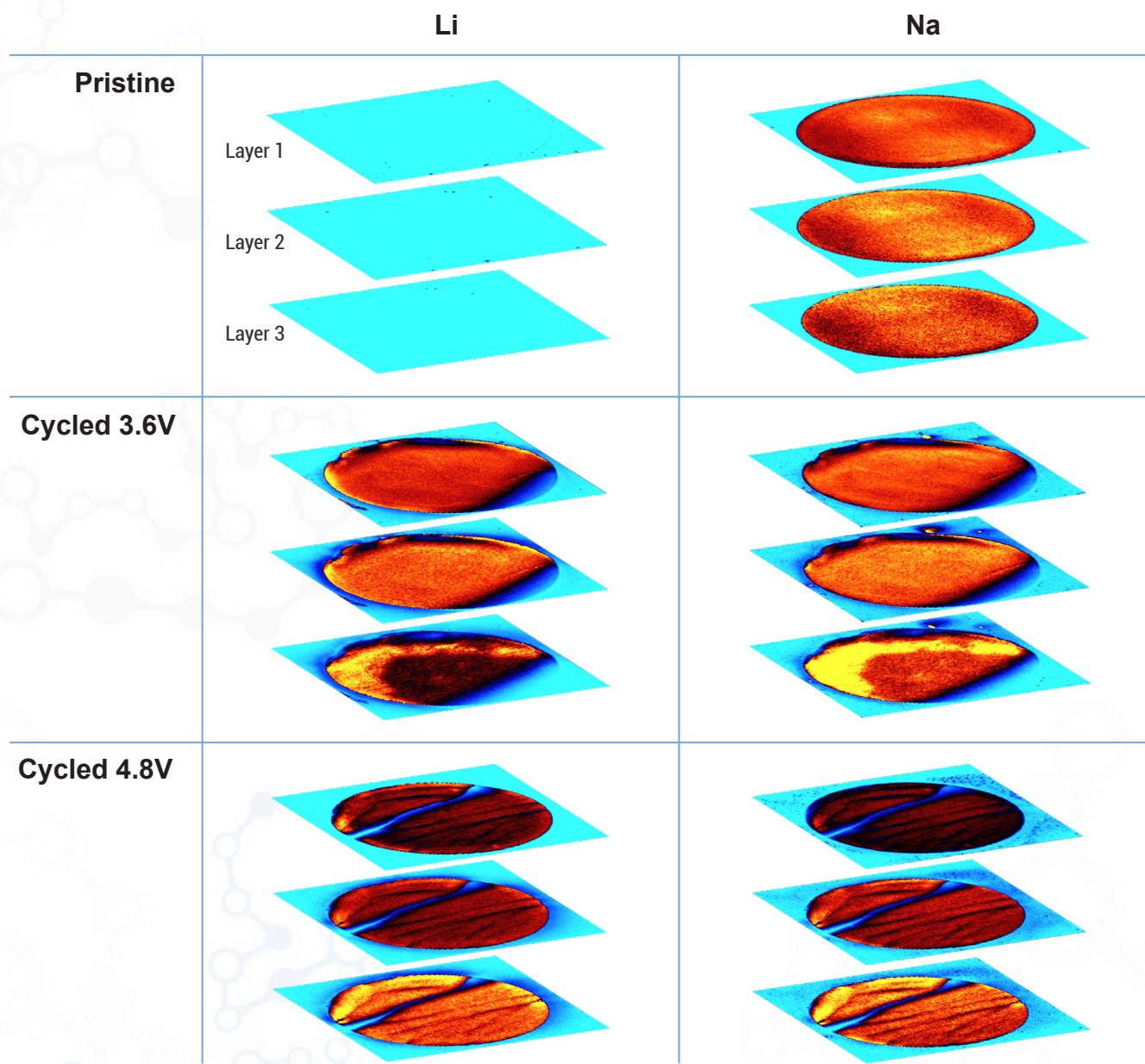

Figure 6. 3D representation of the Li, C, Na, and Ni responses for the pristine, 3.6V, and 4.8V anodes.
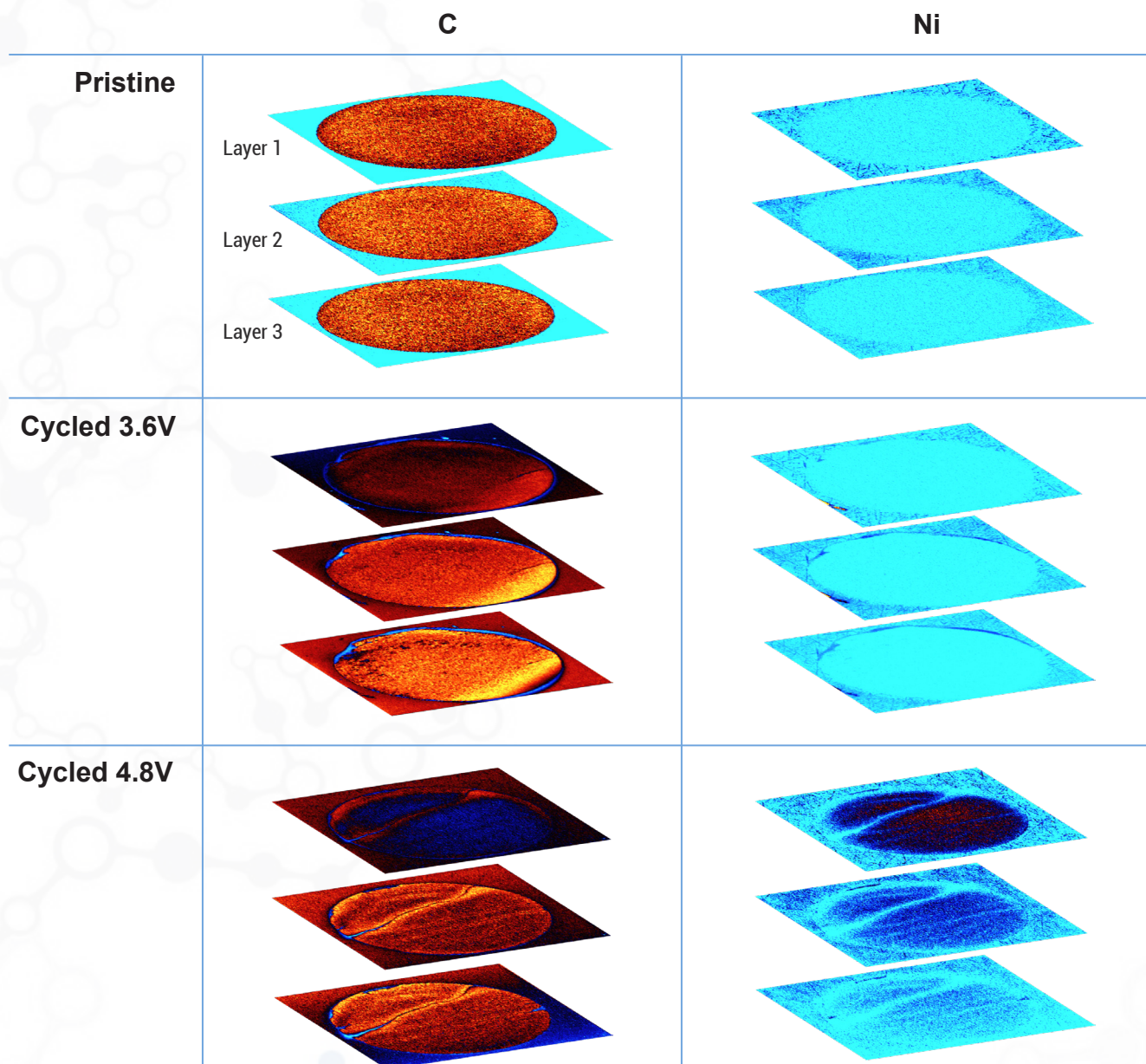
Figure 6 (continued). 3D representation of the Li, C, Na, and Ni responses for the pristine, 3.6V, and 4.8V anodes.
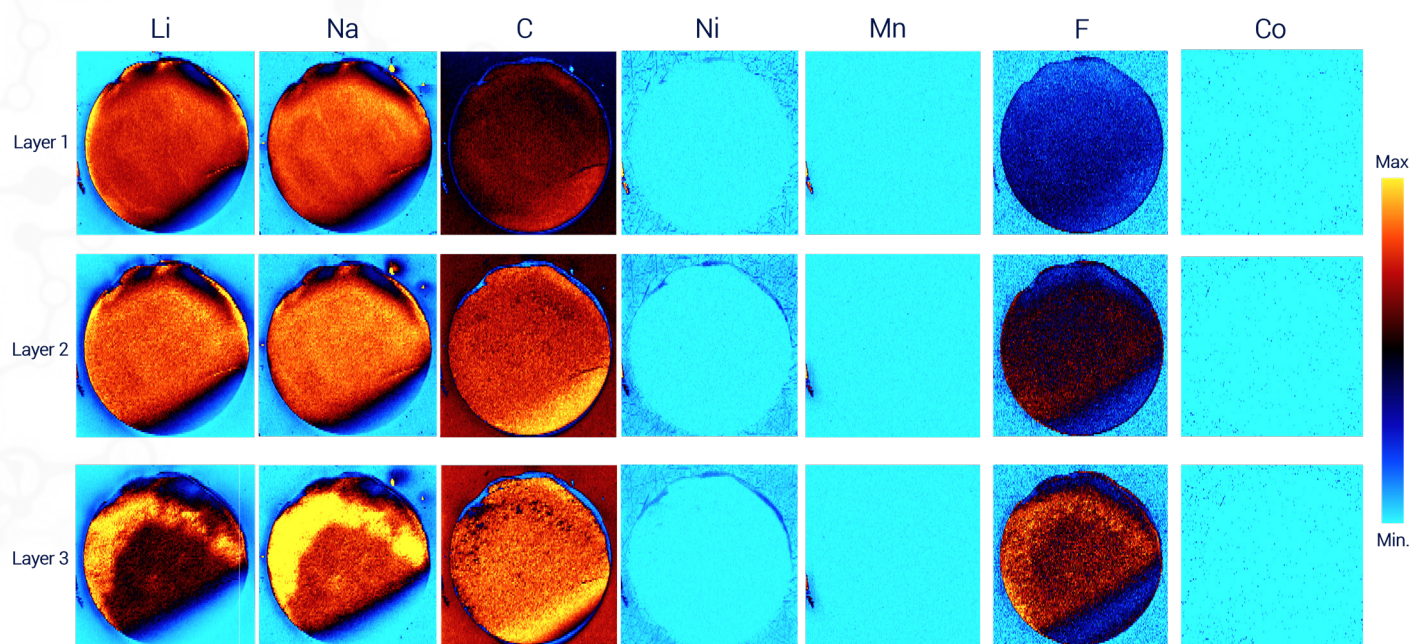
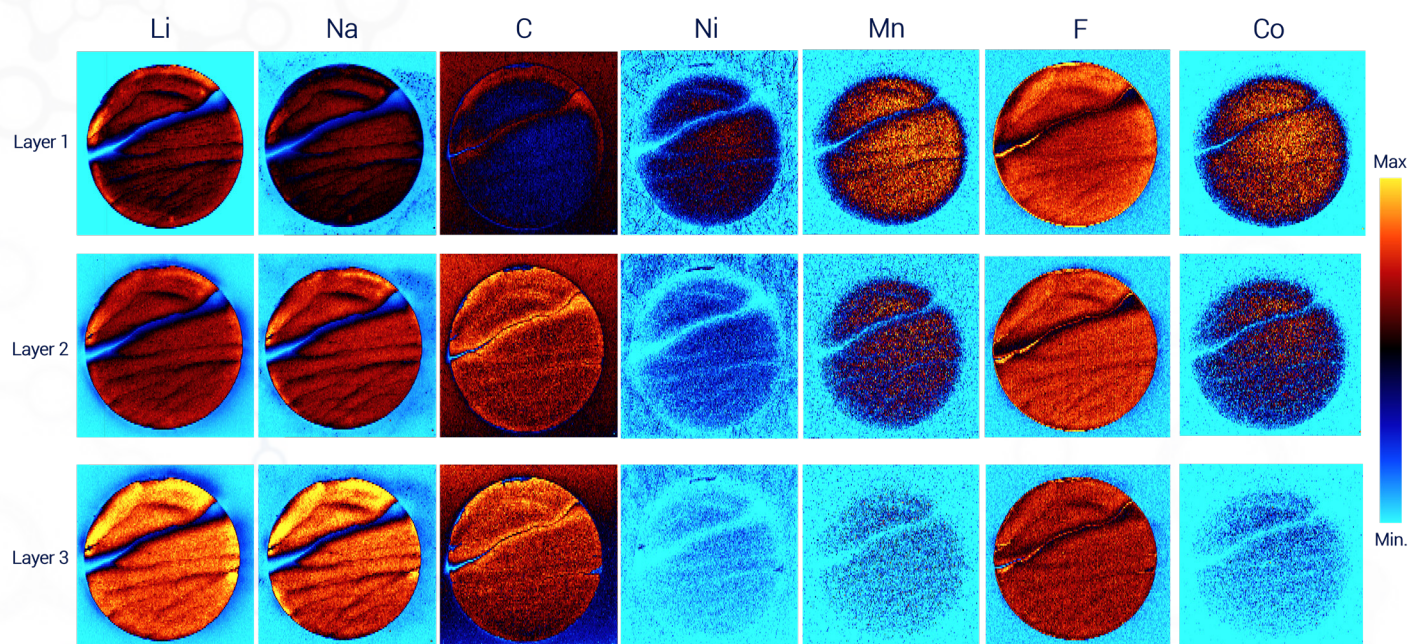Figure 7. Elemental maps of layers 1, 2, and 3 for the 3.6V anode.

Figure 8. Elemental maps of layers 1, 2, and 3 for the 4.8V anode.

One set of the anodes cycled at 3.6V were constructed with and without FEC added to the electrolyte. Figure 9 displays the comparison of F response from the two anodes. The anode without FEC shows a slightly higher F response on the surface (likely from the $LiPF_6$ electrolyte) but decreases when getting deeper into the anode. It is expected that F would be detected throughout, since PVDF binder was used with the graphite material to construct the anode. The FEC anode had higher F responses as you get closer to the Cu collector, which suggests that the SEI layer was just beneath a film created during the cycling of the battery. Therefore, the detection of F was only possible after some laser pulses removed this layer reaching the SEI. The F response for these anodes was collected with the iLumen, while the rest of the elements displayed in this work came from the ESLumen. Figure 10 shows the comparison of the LIBS spectra from the 3.6V anodes with and without FEC.
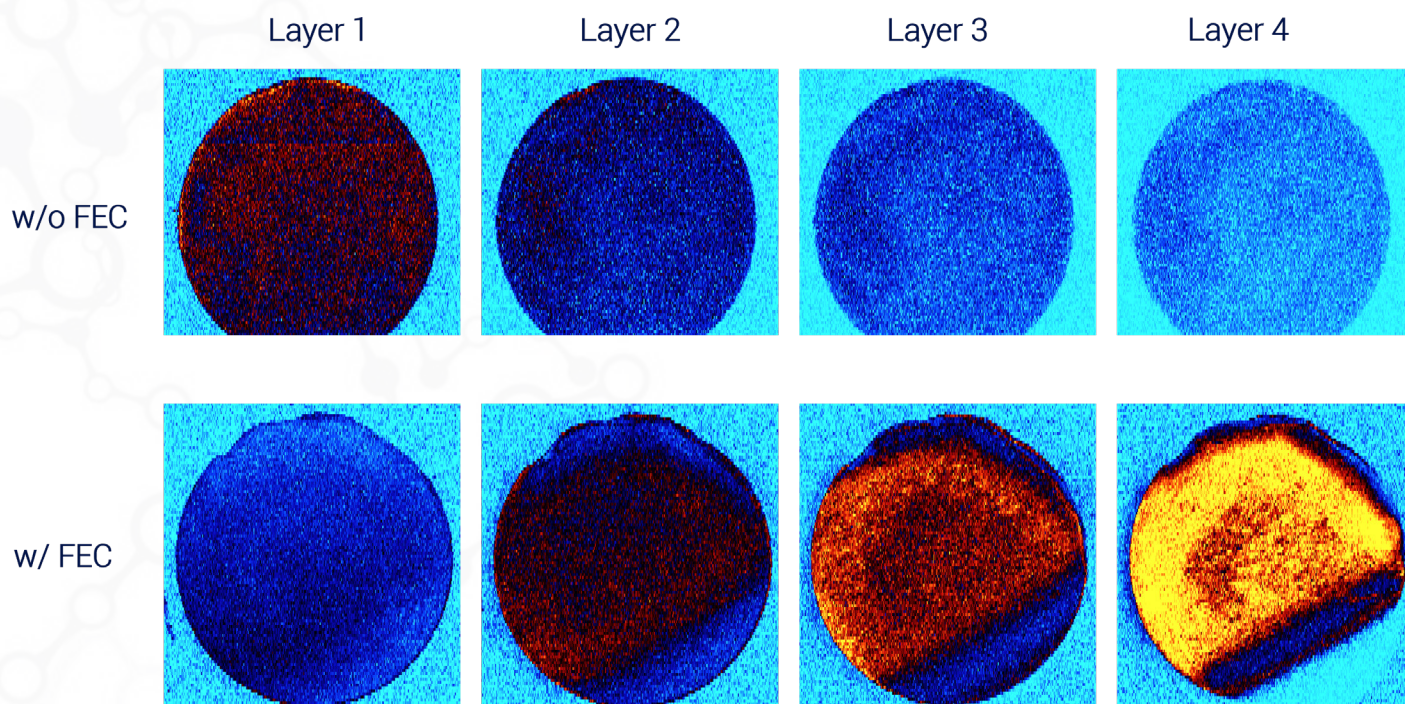

Figure 9. Comparison of the F response by layer for the 3.6V anode with and without FEC.
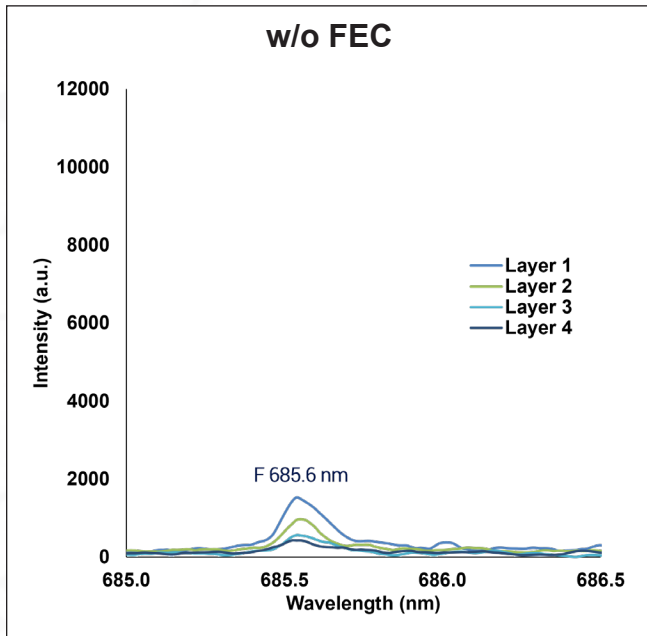
w/o FEC

F 685.6 nm

Figure 9. Comparison of the F response by layer for the 3.6V anode with and without FEC.
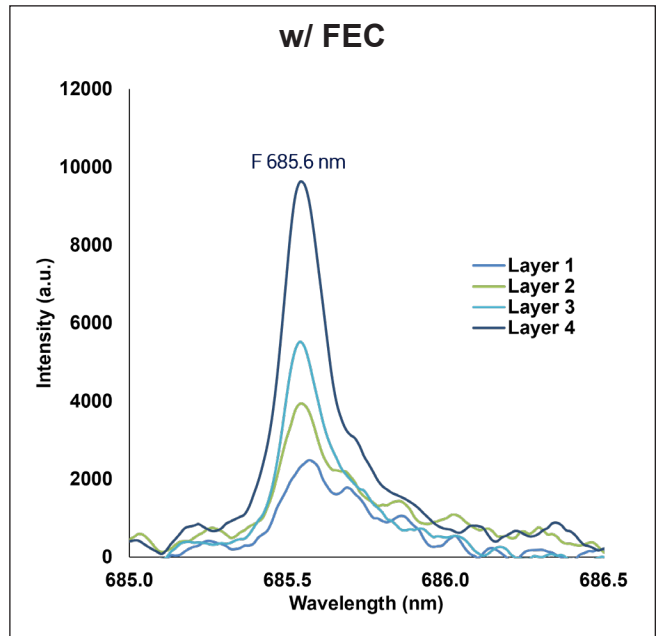

w/ FEC

F 685.6 nm

Figure 10. LIBS spectra overlapped from the iLumen comparing the F response of the 3.6V anode with and without FEC.

Conclusions

LIBS was used to successfully analyze and image elemental distributions in anode materials. The ESLumen was used to collect broadband LIBS spectra which provided elemental information for C, Li, Na, O, Ni, Mn, and Co. While the iLumen was used to gain increased sensitivity for F. After cycling an SEI layer is formed on the surface of the 3.6V and 4.8V anodes, this was easily discernable in the data with the lower response of C and Na on the surface layers. In addition, the overcycling to 4.8V showed the addition of Ni, Mn, Co, and O on the anode surface from the $LiNiMnCoO_2$ cathode material. The imageGEO^{LIBS} system provides an elemental analysis tool capable of providing both elemental distribution and depth information for battery related materials.